

SHAPE OPTIMIZATION FOR LINEAR ELASTIC STRUCTURES USING SENSITIVITY ANALYSIS AND FINITE ELEMENT METHOD

LE VAN CHIEN, NGUYEN HOANG LINH, TA THI THANH MAI
School of Applied Mathematics and Informatics, Hanoi University of Science and Technology

ABSTRACT. In this article, we propose a numerical method for two-dimensional geometrical shape optimization problem in the context of structures of linear elasticity. Our approach is based on a combination of the classical shape derivative and Hadamard's boundary variation method. The shape derivative is computed by Lagrange's approach via the solution to the state and adjoint equations. In addition to the use of moving mesh according to the descent direction, the proposed algorithm also necessitates topological gradient resmoothing techniques. Its convergence to a (local) minimum, illustrated by several numerical experiments in the contexts of structural mechanics with the objective function of compliance and volume constraint.

Keywords: Shape optimization, sensitivity analysis, shape derivative, linear elastic structure, Freefem++.

1 Introduction

Shape optimization in general and shape optimization of elastic structures has received a lot of attentions from mathematicians and engineers alike.

Many approaches have been studied extensively over the years and have brought forth interesting results in theory and in applications. Among numerous methods introduced to solve the structural optimization problems at hands, the representation of the shapes and the computation of the sensitivity of the objective criterion with respect to the design are perhaps the two distinguishing factors.

The oldest and most popular one, the classical shape optimization method [17, 20], is based on the computation of the sensitivity of the criterion of interest with respect to a smooth variation of the boundary. Its main drawback is that it does not allow any topology changes.

To overcome this limitation, relaxed formulations using e.g. the homogenization theory have been introduced [3, 1, 7]. Considering the number of publications, these approaches and their variants (power-law method or solid isotropic microstructure with penalization method) are quite classical, see [6, 5, 7, 3, 1] for examples. This class of methods is called the *density methods*. By defining a density function θ whose value range from 0 to 1 over a computational domain D , the shape optimization problem is posed as a parametric optimization problem, which is solved by optimizing the distribution of the mixture of material and void in the computational. The value of θ is close to 0 if there is almost only void, and close to 1 if there is almost only the shape.

However, these methods are mainly restricted to linear elasticity and particular objective functions. Despite their high computational cost, stochastic algorithms (like genetic algorithms, see e.g. [15]) can be used to deal with more general situations, or when practical reasons make difficult a sensitivity computation (for instance the adjoint state may not be easily computable).

Aside from density methods, *implicit methods* have also been studied and developed. Interface-tracking or interface-capturing techniques in finite element computation utilize them extensively. The most popular in shape-topology optimization of them is the *level set method*. Notable examples include Wang et al. with a topology optimization method for linearly elastic structures using an implicit moving boundary [22], or Allaire et al. with a structural optimization method based on a combination of shape derivative and the level set method for front propagation in [4].

In this article, we aim to construct a numerical scheme for the problem of shape optimization in linear elasticity structure. We discuss the situation here to illustrate our ideas: Let $\Omega \in \mathbb{R}^d (d = 2 \text{ or } 3)$ be a bounded open set occupied by a linear isotropic elastic material governed by the elastic equations (the static equilibrium equations (1) which will be considered in detail in the next section):

$$\begin{cases} -\operatorname{div}(Ae(u)) &= f & \text{in } \Omega, \\ u &= 0 & \text{on } \Gamma_D, \\ (Ae(u))n &= g & \text{on } \Gamma_N, \\ (Ae(u))n &= 0 & \text{on } \Gamma. \end{cases}$$

The problem is to minimize an objective function denoted by $J(\Omega)$ which depends on the domain Ω via the solution u_Ω of elastic system where the variable shape Ω belongs to a set of admissible shapes \mathcal{U}_{ad} .

Formally speaking, our model of shape optimization is:

$$\inf_{\Omega \in \mathcal{U}_{\text{ad}}} J(\Omega).$$

From the numerical point of view, shapes are represented via a computational mesh, on which the elastic equations are solved. In our approach, the deformation of shape Ω is achieved by moving the vertices of the mesh according to the descent direction.

The direction is computed using the shape derivative, by means of an adjoint problem. However, unlike the approach in [4] using the so-called "ersatz material" which amounts to fill the holes by a weak phase, we only need to impose the state and adjoint problems on the computational shape. In the setting of elastic equations, we optimize shapes with the objective function of compliance under the volume constraints. It is achieved thanks to the Lagrangian - like algorithm based on the first order derivative of shape which will be discussed in details in section 4.

This is a continuation of our previous work in fluid mechanics shape optimization [21, 16]. We also refer to [11] for more exhaustive study on this topic. Naturally, in the context of many other complex physics problems such as thermoelasticity, heat conduction,... this method also proves efficient to a large extent. For this reason, we have made available our source code at:

Any suggestions or contributions are welcome.

This paper is organized into five sections. Section 2 provides a brief description of the optimization problem for linear elasticity problem. Section 3 reviews some classical theories of shape sensitivity analysis based on Hadamard's boundary variation method. Section 4 is the central section. It presents the computation of the objective function's derivative, as well as the descent direction; the details of our algorithm is outlined in Section 4.4. The numerical test cases are presented in Section 5. Section 6 gives some perspectives and comments about the effectiveness and limitations of the scheme.

2 Setting of the problem

Consider a bounded domain $\Omega \in \mathbb{R}^d (d = 2 \text{ or } 3)$ occupied by a linear isotropic elastic material with Hooke's law A . The boundary of Ω is made of three disjoint parts:

$$\partial\Omega = \Gamma_N \cup \Gamma_D \cup \Gamma,$$

where Γ_N is the Neumann boundary, Γ_D is the Dirichlet boundary and Γ the free moving boundary. We shall see that only the free moving boundary Γ is

subject to optimization.

If Ω is held stationary on Γ_D , let f be the vector-valued function of the volume forces defined over every points in Ω and g be the surface loads. The displacement field u in Ω is the solution to the linearized elasticity system:

$$\begin{cases} -\operatorname{div}(Ae(u)) &= f & \text{in } \Omega, \\ u &= 0 & \text{on } \Gamma_D, \\ (Ae(u))n &= g & \text{on } \Gamma_N, \\ (Ae(u))n &= 0 & \text{on } \Gamma, \end{cases} \quad (1)$$

which is the static equilibrium equations for u . A and e are defined by:

$$\begin{aligned} A\psi &= 2\mu\psi + \lambda(\operatorname{Tr}\psi)\operatorname{Id}, \\ e(u) &= \frac{1}{2}(\nabla u^T + \nabla u), \end{aligned}$$

where μ and λ are the Lámé module of the material, which are calculated from the Young modulus E and the Poisson's ratio ν by these formulas:

$$\begin{aligned} \mu &= \frac{E}{2(1+\nu)}, \\ \lambda &= \frac{E\nu}{(1+\nu)(1-2\nu)}. \end{aligned}$$

Physically speaking A is the stress (the internal forces that neighboring particles of a continuous material exert on each other) and e is the strain in the material (the deformation). While Ω changes over the optimization process,

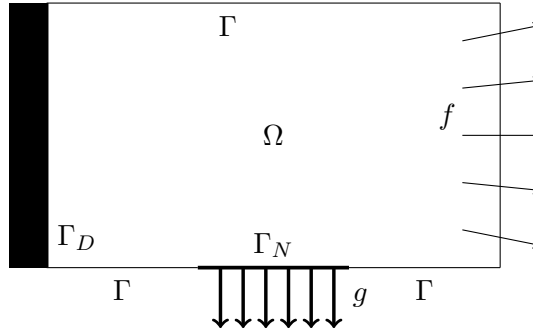


Figure 1: *Setting of the problem of optimization in elastic structures*

it is necessary to know f and g for all possible configurations. The set of all admissible shapes is defined as:

$$\mathcal{U}_{\text{ad}} = \{\Omega \text{ bounded and Lipschitz, } \Gamma_N \cup \Gamma_D \subset \partial\Omega\}.$$

As stated, we aim to minimize an objective function which depends on the domain Ω via the solution u_Ω of elastic system where the variable shape Ω belongs to a set of admissible shapes \mathcal{U}_{ad} .

The first choice that comes to mind is the classic compliance which shall be our main objective function of interest:

$$J_1(\Omega) = \int_{\Omega} f \cdot u dx + \int_{\Gamma_N} g \cdot u ds = \int_{\Omega} Ae(u) : e(u) dx. \quad (2)$$

Another choice is the least - square error:

$$J_2(\Omega) = \int_{\Omega} |u - u_0|^2 dx. \quad (3)$$

3 Shape representation and derivatives

One particularly popular method for describing the variations of a shape is Hadamard's boundary variation method.

3.1 Shape sensitivity analysis by Hadamard method

Hadamard's boundary variation's core idea was proposed in the seminal paper [13] (see also [20]) and later meticulously employed in [18]. Here, following the approach of Murat [18] and Simon [19], we consider the variation of a given smooth reference shape Ω according to the displacement θ :

$$(I + \theta)(\Omega)$$

with $\theta \in W^{1,\infty}(\mathbb{R}^d, \mathbb{R}^d)$ (see figure 2). It is well known that, for sufficiently small θ , $(I + \theta)(\Omega)$ is a diffeomorphism in \mathbb{R}^d .

Before going into more details of the Hadamard's method, it is important that we define the set of all admissible variations in our shape optimization scheme:

$$\Theta_{\text{ad}} = \{\theta \in W^{1,\infty}(\mathbb{R}^d, \mathbb{R}^d), \theta = 0 \text{ on } \Gamma_N \cup \Gamma_D\}.$$

In the context of Hadamard's method, the variations $(I + \theta)(\Omega)$ of Ω only depend on the values taken by θ on $\partial\Omega$, and we have the following consequence of Picard's fixed point theorem (see lemma 6.13 in [2] for a proof):

Lemma 1. *For every deformation field $\theta \in W^{1,\infty}(\mathbb{R}^d, \mathbb{R}^d)$ such that $\|\theta\|_{W^{1,\infty}(\mathbb{R}^d, \mathbb{R}^d)} < 1$, the application $(I + \theta) : \mathbb{R}^d \rightarrow \mathbb{R}^d$ is a Lipschitz homeomorphism with Lipschitz inverse.*

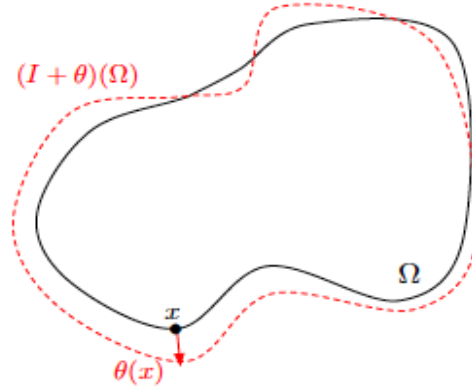


Figure 2: Variation $I + \theta$ of a reference shape Ω .

Let $\Omega \subset \mathbb{R}^d$ be a fixed domain, for which Lipschitz regularity holds. For any $\theta \in W^{1,\infty}(\mathbb{R}^d, \mathbb{R}^d)$ satisfying $\|\theta\|_{W^{1,\infty}(\mathbb{R}^d, \mathbb{R}^d)} < 1$, we denote by $\Omega_\theta := (I + \theta)(\Omega)$ the deformed shape with respect to θ .

Note that $W^{1,\infty}(\mathbb{R}^d, \mathbb{R}^d) \subset L^\infty(\mathbb{R}^d)^d$ is the Banach space of bounded functions $\theta : \mathbb{R}^d \rightarrow \mathbb{R}^d$, equipped with the natural norm:

$$\forall \theta \in W^{1,\infty}(\mathbb{R}^d, \mathbb{R}^d), \|\theta\|_{W^{1,\infty}(\mathbb{R}^d, \mathbb{R}^d)} := \|\theta\|_{L^\infty(\mathbb{R}^d)^d} + \|\nabla \theta\|_{L^\infty(\mathbb{R}^d)^{d \times d}}.$$

Hence, variations of a given shape Ω are parametrized by an open subset of a Banach space. This allows us to rewrite operations performed on Ω in the form using the underlying deformation field θ and enabled the introduction of shape differentiability.

3.2 Shape differentiability

In order to apply a gradient method to the minimization problem in Section 2, we recall classical definition of shape derivative and results about the differentiation with respect to the domain of functionals of type: $\Omega \mapsto J(\Omega) \in \mathbb{R}$.

Definition 1. Let $J(\Omega)$ be a functional of the domain. J is shape differentiable at Ω if the underlying application:

$$\begin{aligned} W^{1,\infty}(\mathbb{R}^d, \mathbb{R}^d) &\longrightarrow \mathbb{R} \\ \theta &\longmapsto J(\Omega_\theta) \end{aligned}$$

is Fréchet differentiable at $\theta = 0$. The associated Fréchet differential, denoted $J'(\Omega)$, is called the shape derivative of J at Ω . We have following expansion

in the vicinity of $0 \in W^{1,\infty}(\mathbb{R}^d, \mathbb{R}^d)$:

$$J(\Omega_\theta) = J(\Omega) + J'(\Omega)(\theta) + o(\theta), \quad \text{with } \lim_{\theta \rightarrow 0} \frac{|o(\theta)|}{\|\theta\|} = 0. \quad (4)$$

Remark 1.

1. $J'(\Omega)$ is a continuous linear form on $W^{1,\infty}(\mathbb{R}^d, \mathbb{R}^d)$.
2. In the case of a functional which also depends on other variables than Ω , the partial Fréchet differential with respect to the domain is denoted as $\frac{\partial}{\partial \Omega}$.

A classical result states that the directional derivative $J'(\Omega)(\theta)$ depends only on the normal trace $\theta \cdot n$ (n is the normal unit vector field to Ω) on the boundary $\partial\Omega$, see [4].

Lemma 2. Let Ω be a smooth bounded open set and $J(\Omega)$ a differentiable function at Ω . If $\theta_1, \theta_2 \in W^{1,\infty}(\mathbb{R}^d, \mathbb{R}^d)$ satisfy $\theta_2 - \theta_1 \in \mathbb{C}(\mathbb{R}^d, \mathbb{R}^d)$ and $\theta_1 \cdot n = \theta_2 \cdot n$, then we have:

$$J'(\Omega)(\theta_1) = J'(\Omega)(\theta_2).$$

We also recall here two results on shape derivative that will be used in computing the shape derivatives in the sequence. (see [14] or [4] for the proofs).

Lemma 3. Let Ω be a bounded Lipschitz domain and let $f(x) \in W^{1,1}(\mathbb{R}^d)$. If $J(\Omega) = \int_{\Omega} f(x) dx$ is a differentiable function at Ω then we have

$$J'(\Omega)(\theta) = \int_{\Omega} \operatorname{div}(\theta f) dx = \int_{\partial\Omega} f \theta \cdot n ds$$

for any $\theta \in W^{1,\infty}(\mathbb{R}^d, \mathbb{R}^d)$.

Lemma 4. Let Ω be a bounded Lipschitz domain in class \mathbb{C}^2 and $g(x) \in W^{2,1}(\mathbb{R}^d)$, κ be the curvature of shape defined as $\kappa = \operatorname{div} n$. If $J(\Omega) = \int_{\partial\Omega} g(x) ds$ is a differentiable function at Ω , and

$$J'(\Omega)(\theta) = \int_{\partial\Omega} \left(\frac{\partial g}{\partial n} + \kappa g \right) \theta \cdot n ds$$

for any $\theta \in W^{1,\infty}(\mathbb{R}^d, \mathbb{R}^d)$. Furthermore, this result still holds true if one replaces $\partial\Omega$ by Γ , a smooth open subset of $\partial\Omega$, and assumes that $g = 0$ on the surface boundary of Γ .

Remark 2. In particular, Lemma 3 is useful in order to compute the shape derivative of a volume constraint $V(\Omega) = C$. Indeed, we have:

$$V(\Omega) = \int_{\Omega} dx \quad \text{and} \quad V'(\Omega)(\theta) = \int_{\partial\Omega} \theta \cdot n ds. \quad (5)$$

Similarly, Lemma 4 is useful in order to compute the shape derivative of a perimeter constraint $P(\Omega) = C$ since we have:

$$P(\Omega) = \int_{\partial\Omega} ds \quad \text{and} \quad P'(\Omega)(\theta) = \int_{\partial\Omega} \kappa\theta \cdot n ds. \quad (6)$$

4 The shape optimization algorithm

4.1 Computation of the derivatives

It is by no mean an easy task to compute the derivatives of the objective functions mentioned in section 2, especially the compliance. To obtain the derivatives of such functions, we use the C ea's fast derivation method, introduced in [9]. Assume that all the admissible shapes, deformation fields and displacement functions u are smooth enough, and let $j, l : \mathbb{R}^d \times \mathbb{R}^d \rightarrow \mathbb{R}$ be two smooth functions. Consider a general objective function:

$$J(\Omega) = \int_{\Omega} j(u) dx + \int_{\Gamma \cup \Gamma_N} l(u) ds. \quad (7)$$

For the compliance objective function, $j(u) = f \cdot u$ and $l(u) = g \cdot u$.

Theorem 1. $J(\Omega)$ of the form (7) is shape differentiable at any $\Omega \in \mathcal{U}_{ad}$ and its shape derivative reads:

$$\begin{aligned} J'(\Omega)(\theta) = & \int_{\Gamma \cup \Gamma_N} \theta \cdot n \left(j(u) + Ae(u) : e(p) - p \cdot f + \kappa l(u) + \frac{\partial l(u)}{\partial n} \right) ds \\ & - \int_{\Gamma_N} \theta \cdot n \left(\kappa g \cdot p + \frac{\partial (g \cdot p)}{\partial n} \right) ds + \int_{\Gamma_D} \theta \cdot n (j(u) + Ae(u) : e(p)) ds, \end{aligned} \quad (8)$$

where $p \in (H_{\Gamma_D}^1(\Omega))^d$ is the adjoint state, defined as the unique solution to the system:

$$\begin{cases} -\operatorname{div}(Ae(p)) & = -j'(u) & \text{in } \Omega, \\ p & = 0 & \text{on } \Gamma_D, \\ (Ae(p)) n & = -l'(u) & \text{on } \Gamma_N \cup \Gamma. \end{cases} \quad (9)$$

Proof: We consider a general objective function:

$$J(\Omega) = \int_{\Omega} j(u_{\Omega}(x)) dx + \int_{\Gamma \cup \Gamma_N} l(u_{\Omega}(x)) ds.$$

The Lagrange function can be constructed as:

$$\begin{aligned} \mathcal{L}(\Omega, u, p) &= \int_{\Omega} j(u) dx + \int_{\Gamma \cup \Gamma_N} l(u) ds + \int_{\Omega} (Ae(u) : e(p) - p \cdot f) dx \\ &\quad - \int_{\Gamma_N} p \cdot g ds - \int_{\Gamma_D} (p \cdot Ae(u)n + u \cdot Ae(p)n) ds. \end{aligned}$$

The partial derivatives of \mathcal{L} with respect to the each variable read:

$$\begin{aligned} \left\langle \frac{\partial \mathcal{L}}{\partial p}(\Omega, u, p), \bar{u} \right\rangle &= \int_{\Omega} (Ae(u) : e(\bar{u}) - \bar{u} \cdot f) dx - \int_{\Gamma_N} \bar{u} \cdot g ds \\ &\quad - \int_{\Gamma_D} (\bar{u} \cdot Ae(u)n + u \cdot Ae(\bar{u})n) ds \\ &= - \int_{\Omega} \bar{u} \cdot (\operatorname{div}(Ae(u)) + f) dx + \int_{\Gamma_N} \bar{u} \cdot (Ae(u)n - g) ds \\ &\quad + \int_{\Gamma} \bar{u} \cdot Ae(u)n ds - \int_{\Gamma_D} u \cdot Ae(\bar{u})n ds. \\ \left\langle \frac{\partial \mathcal{L}}{\partial u}(\Omega, u, p), \bar{p} \right\rangle &= \int_{\Omega} j'(u) \cdot \bar{p} dx + \int_{\Gamma \cup \Gamma_N} l'(u) \cdot \bar{p} ds + \int_{\Omega} Ae(\bar{p}) : e(p) dx \\ &\quad - \int_{\Gamma_D} (p \cdot Ae(\bar{p})n + \bar{p} \cdot Ae(p)n) ds \\ &= \int_{\Omega} (j'(u) - \operatorname{div}(Ae(p))) \cdot \bar{p} dx + \int_{\Gamma_N \cup \Gamma} (Ae(u)n + l'(u)) \cdot \bar{p} ds \\ &\quad - \int_{\Gamma_D} (p \cdot Ae(\bar{p})n) ds. \end{aligned}$$

It has been observed that the equilibrium of $\frac{\partial \mathcal{L}}{\partial p}(\Omega, u, p)$ yields the variational formulation associated to the state system. There exists a unique solution u_{Ω} of the weak form of the state system and it can be easily verified that:

$$J(\Omega) = \mathcal{L}(\Omega, u_{\Omega}, p), \quad \forall p \in H_{\Gamma_D}^1(\mathbb{R}^d)^d.$$

By taking the partial derivative of two parts with respect to domain Ω , we have:

$$J'(\Omega)(\theta) = \frac{\partial \mathcal{L}}{\partial \Omega}(\Omega, u_{\Omega}, p)(\theta) + \frac{\partial \mathcal{L}}{\partial u}(\Omega, u_{\Omega}, p)u'_{\Omega}(\theta). \quad (10)$$

Hence, if p_{Ω} are solutions of the system of $\frac{\partial \mathcal{L}}{\partial u}(\Omega, u_{\Omega}, p) = 0$ which is also called adjoint system written as follows:

$$\begin{cases} -\operatorname{div}(Ae(p)) & = -j'(u) & \text{in } \Omega, \\ p & = 0 & \text{on } \Gamma_D, \\ (Ae(p))n & = -l'(u) & \text{on } \Gamma_N \cup \Gamma, \end{cases} \quad (11)$$

then the partial differential of objective function with respect to domain Ω can be formulated in a rather simple way:

$$J'(\Omega)(\theta) = \frac{\partial \mathcal{L}}{\partial \Omega}(\Omega, u_\Omega, p_\Omega)(\theta). \quad (12)$$

Applying Lemma 3, Lemma 4, we have the shape derivative of the objective function in this case:

$$\begin{aligned} J'(\Omega)(\theta) &= \int_{\partial\Omega} \theta \cdot n (j(u) + Ae(u) : e(p) - p \cdot f) ds + \int_{\Gamma \cup \Gamma_N} \theta \cdot n \left(\kappa l(u) + \frac{\partial l(u)}{\partial n} \right) ds \\ &\quad - \int_{\Gamma_N} \theta \cdot n \left(\kappa g \cdot p + \frac{\partial(g \cdot p)}{\partial n} \right) ds - \int_{\Gamma_D} \theta \cdot n \left(\kappa h + \frac{\partial h}{\partial n} \right) ds. \end{aligned} \quad (13)$$

with $h = p \cdot Ae(u)n + u \cdot Ae(p)n$. Noting that $u = p = 0$ on Γ_D , we have:

$$\begin{aligned} J'(\Omega)(\theta) &= \int_{\Gamma \cup \Gamma_N} \theta \cdot n \left(j(u) + Ae(u) : e(p) - p \cdot f + \kappa l(u) + \frac{\partial l(u)}{\partial n} \right) ds \\ &\quad - \int_{\Gamma_N} \theta \cdot n \left(\kappa g \cdot p + \frac{\partial(g \cdot p)}{\partial n} \right) ds + \int_{\Gamma_D} \theta \cdot n (j(u) + Ae(u) : e(p)) ds. \end{aligned} \quad (14)$$

The proof of Theorem 1 has been accomplished.

If the objective function is the compliance, i.e. $j(u) = f \cdot u$, $l(u) = g \cdot u$ on Γ_N and $l(u) = 0$ on Γ , it is easy to see that $p = -u$ and the problem is self-adjoint. In this case, the shape derivative of the compliance objective function reads:

$$\begin{aligned} J'(\Omega)(\theta) &= \int_{\Gamma_N} \theta \cdot n \left(2 \left(u \cdot f + \kappa g \cdot u + \frac{\partial(g \cdot u)}{\partial n} \right) - Ae(u) : e(u) \right) ds \\ &\quad + \int_{\Gamma} \theta \cdot n (2u \cdot f - Ae(u) : e(u)) ds - \int_{\Gamma_D} \theta \cdot n Ae(u) : e(u) ds. \end{aligned} \quad (15)$$

4.2 The Lagrangian - like algorithm

In industrial context, a lot of demanding constraints may arise, such as volume, perimeter, curvature of shapes,... so that while the compliance is optimized, the shape retains practicality and doesn't impose a lot of difficulty in

manufacturing. However, within the scope of this paper, we shall only limit ourselves to the volume constraints.

The optimization problem is brought back to that of the constraints - free minimization of a weighted sum of $J(\Omega)$ and $V(\Omega)$, the latter being penalized with a fixed positive Lagrange multiplier l :

$$\inf_{\Omega \in \mathcal{U}_{\text{ad}}} \mathcal{L}(\Omega), \quad \mathcal{L}(\Omega) = (J(\Omega) + lV(\Omega)). \quad (16)$$

Also, it is known that for the optimization problem posed as (16), there exists at least one optimal solution (see [4]).

Algorithm 1: Lagrangian - like algorithm

$n = 0$, start with an initial guess Ω^0 and multiplier l .

for $n = 1, 2, \dots$ *until convergence* **do**

1. Infer a descent direction θ^n for $\mathcal{L}(\Omega)$.
2. Choose a descent step $\tau^n > 0$ small enough so that $\mathcal{L}((Id + \tau^n \theta^n)\Omega^n) < \mathcal{L}(\Omega^n)$.
3. Set $\Omega^{n+1} = \Omega_{\tau^n \theta^n}^n$.

end

4.3 Computation the descent direction

Given a shape $\Omega \in \mathcal{U}_{\text{ad}}$, the form

$$\mathcal{L}'(\Omega)(\theta) = \int_{\partial\Omega} \phi_{\Omega} \theta \dot{n} ds$$

of the shape derivative of the Lagrange - like function is calculated in accordance to 3.2, Section 4.1.

For any scalar field ϕ_{Ω} , this suggests an immediate choice for a descent direction $\theta(x) \in \Theta_{\text{ad}}$:

$$\forall x \in \partial\Omega, \theta(x) = -\phi_{\Omega}(x)n(x). \quad (17)$$

Using the finite element method, we can accurately obtain the solution to the static equilibrium system on the computational mesh T_{Ω} of Ω . Obviously, ϕ_{Ω} is dependent on this solution. However, $\theta(x)$ proved quite impractical as a descent direction for two reasons as stated as below.

- We need to search for a displacement field θ defined in a neighborhood of $\partial\Omega$ rather than just on $\partial\Omega$ like formula (17).

- The numerical stability of the scheme may not be guaranteed or even completely compromised as the scalar field ϕ_Ω depends on the solution to the static equilibrium equations, more specifically the derivatives of such solution and the solution to the adjoint system, which may not be regular.

Adopting a different scalar product instead of canonical one of $L^2(\Gamma)$ in identifying the gradient of \mathcal{L} is an efficient way to address both problems at the same time. We shall see if we can obtain θ in a Hilbert space V of more regular vector fields, defined in Ω , such that:

$$(\theta, \eta)_V = \mathcal{L}'(\Omega)(\eta) = \int_{\partial\Omega} \phi_\Omega \eta \dot{n} ds \quad \forall \eta \in V. \quad (18)$$

The first option is to use the Laplace-Beltrami operator, the role of which is to ensure the considered vector fields sustain regularity, on Γ . Explicitly, let $\alpha > 0$ be a small "extension - regularization" parameter, V is equipped with the inner product:

$$(\theta, \eta)_V = \alpha \int_{\Omega} \nabla \theta : \nabla \eta dx + (1 - \alpha) \int_{\Gamma} \nabla_{\Gamma} \theta : \nabla_{\Gamma} \eta ds \quad (19)$$

where $\nabla_{\Gamma} f := \nabla f - (\nabla f \cdot n)n$ is the tangential gradient of a (smooth) function f . Another idea, presented in [8, 12] is to choose $V = \left\{ v \in H^1(\Omega)^d, v|_{\Gamma_N \cup \Gamma_D} = 0 \right\}$. For this θ is the solution of elliptic system:

$$\begin{cases} -\alpha \nabla \theta + \theta & = 0 & \text{in } \Omega, \\ \theta & = 0 & \text{on } \Gamma_N \cup \Gamma_D, \\ \alpha \frac{\partial \theta}{\partial n} & = \phi_\Omega n & \text{on } \Gamma. \end{cases} \quad (20)$$

This implies that the scalar product in (18) is replaced by:

$$(\theta, \eta)_V = \alpha \int_{\Omega} \nabla \theta : \nabla \eta dx + \int_{\Omega} \theta \cdot \eta dx. \quad (21)$$

Using the asymptotic expansion (4) we can show that θ is still a descent direction for \mathcal{L} (for t small enough: $\mathcal{L}(\Omega_\theta) = \mathcal{L}(\Omega) - t \int_{\Gamma} \phi_+^2 o(t)$). However, θ innately enjoys more regularity than those owing to the classical regularity theory for elliptic equations, and is inherently defined over the whole domain Ω .

4.4 Description of proposed optimization algorithm

We are now in position to outline the proposed general strategy for handling mesh evolution in the context of shape optimization.

Algorithm 2: Shape optimization algorithm

start with an initial guess Ω^0 , multiplier l of Lagrangian - like \mathcal{L} and triangulation mesh T^0 .

for $n = 1, 2, \dots$ *until convergence* **do**

1. Compute displacement u^n of the elasticity system (1) on mesh T^n .
2. Calculate shape gradient ϕ^n of $\mathcal{L}(\Omega^n)$ by using Theorem (1) and Lemma (3), (4).
3. Infer a descent direction θ^n for $\mathcal{L}(\Omega^n)$ by solving equation (21), (19) on the mesh T^n .
4. Choose a descent step $\tau^n > 0$ small enough so that $\mathcal{L}((Id + \tau^n \theta^n)\Omega^n) < \mathcal{L}(\Omega^n)$.
5. Move the vertices of T^n according to θ^n and τ^n .
6. Set $\Omega^{n+1} = \Omega_{\tau^n \theta^n}^n$ and evaluate $J(\Omega^{n+1})$.
if *resulting mesh is valid and* $J(\Omega^{n+1}) < J(\Omega^n)$ **then**
 Ω^{n+1} is retained as the new shape
else
 $\Omega^{n+1} = \Omega^n$.
Go back to Step 4, decreasing the chosen value for the time step.
end

end

5 Numerical examples

In this section, we present our numerical results to the elastic shape optimization model that we have studied. For all tests, the coefficients for the elastic material are $E = 1$ (the Young modulus) and $\nu = 0.3$ (the Poisson ratio). Also, we assume that no body forces are applied ($f = 0$). Under such assumption, the shape derivative of (16) reads simply as:

$$\mathcal{L}'(\Omega) = \int_{\Gamma} (l - Ae(u) : e(u)) \theta \cdot nds.$$

As for regularization of the shape boundary, the choice for the inner product the inner product is (19) with α specified for each case.

5.1 A cantilever

The first test case we consider is a cantilever clamped near its top and bottom left corner. Surface load $g = (0, -1)$ are applied on Γ_N which accounts for a small area located at the center of its right-hand side.

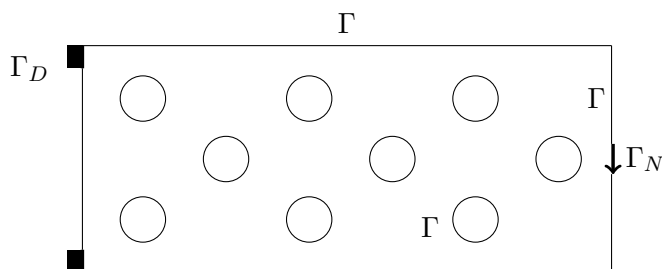


Figure 3: *Model of the cantilever test*

The Lagrange multiplier is set to $l = 12$ and the extension - regularization parameter is set to $\alpha = 0.95$.

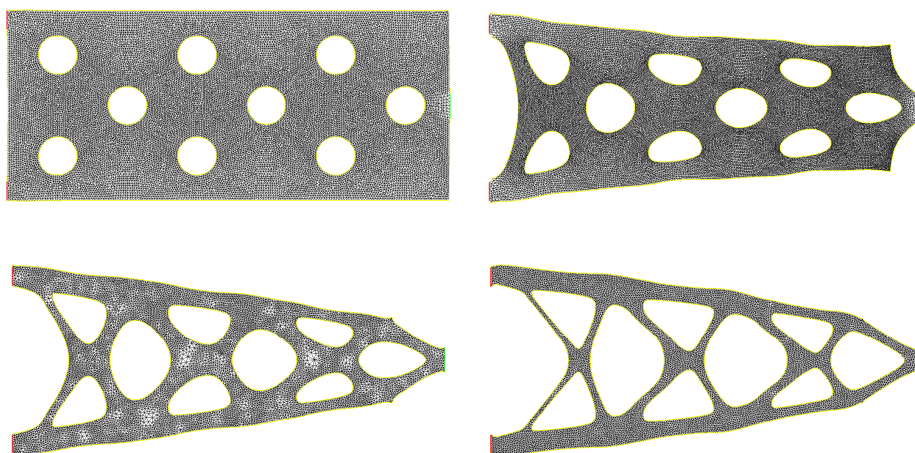


Figure 4: *(From top to bottom) The 1st, 100th, 250th and final iterations of the cantilever test case*

The algorithm converges to a local minimum which strongly depends on the initial guess. By the time of convergence, the shape has been able to achieve regularity as the sharp corners along the edges are no longer present. This

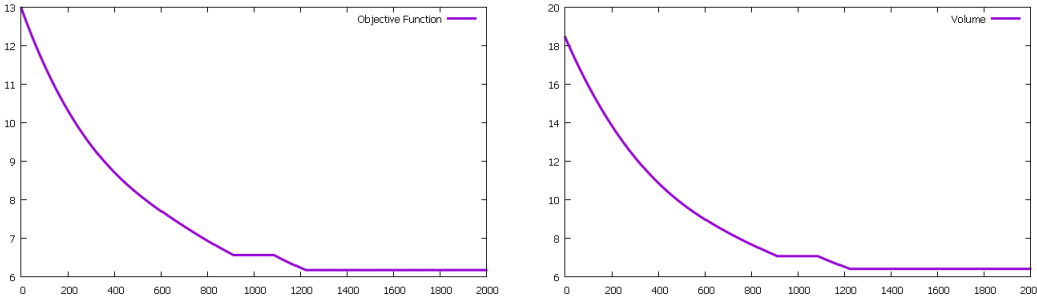
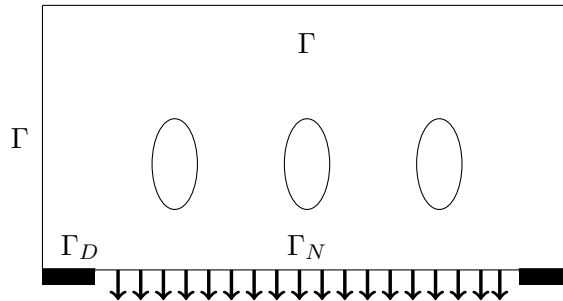


Figure 5: *Convergence history of the objective function and the volume of the cantilever test case*

result seems to be in congruence with the same test case in [4, 10].

5.2 A bridge

The second test case deals with a bridge, whose rigidity is also maximal, just like the cantilever case. The bridge is clamped near its bottom - left and bottom - right corner. Surface loads $g = (0, -1)$ are applied to the bottom side.



The Lagrange multiplier is set to $l = 3$ and the extension - regularization parameter is set to $\alpha = 0.9$.

The algorithm seems to converge much faster this time than the first test case as the optimal shape is obtained only after around 300 iterations. The shape has also been able to achieve regularity as we want it to. This result is in accordance to the one in [10].

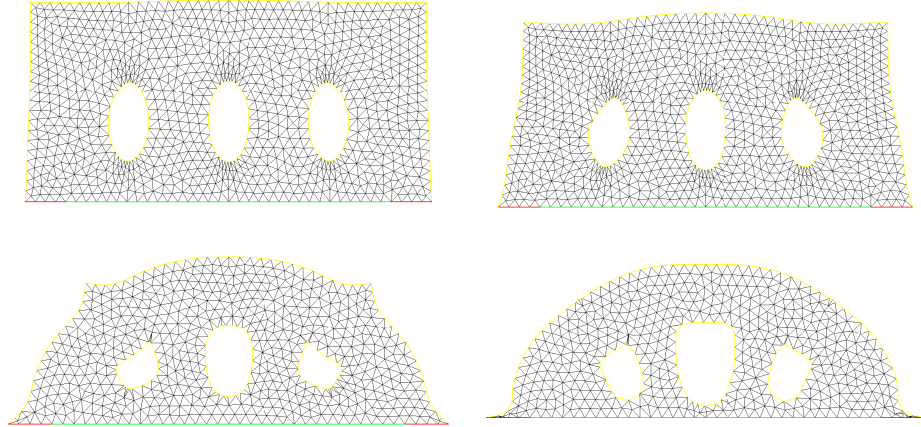


Figure 6: (From top to bottom) The 1st, 40th, 100th and final iterations of the bridge test case

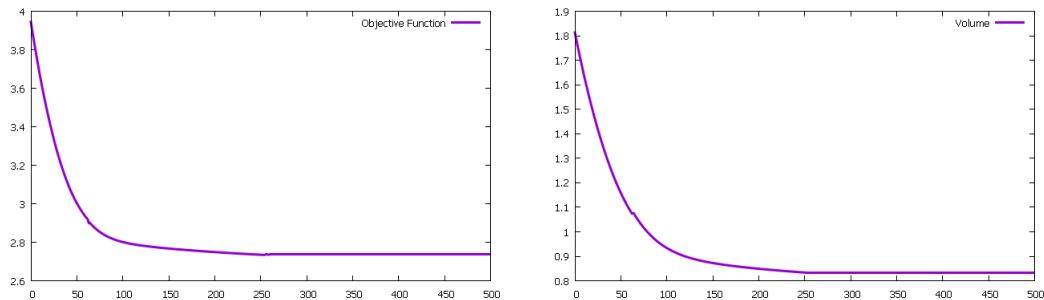


Figure 7: Convergence history of the objective function and the volume of the bridge test case

6 Conclusion and perspectives

We have proposed a numerical scheme for shape optimization in elasticity structure. This algorithm can be extended to deal with other geometric situations, general objective functions and mechanical models, including nonlinear elasticity and design-dependent loads. The efficiency and reliability of present work is assessed by numerical examples in 2D for linear elasticity problems with the minimizing of compliance. The program has been implemented in the FreeFem++ environment. The source code are available online at: <https://github.com/lvchien/shapeoptimization>.

The cost of our numerical algorithm is moderate, however, the resulting optimal

shape is strongly dependent on the initial guess.

Regarding the perspectives, we would like to mention a few options:

- Extend the test cases in 3D with compliance objective function.
- Investigate this scheme with different objective functions (least-square) as suggested in [4, 10].
- Develop an application of the present scheme for shape-topology optimization in other complex physical problems: thermal structure, natural convection, ...

References

- [1] G. ALLAIRE Shape optimization by the homogenization method. Springer Verlag, New York, 2002.
- [2] G. ALLAIRE Conception optimale de structures, Mathematiques et Applications, volume 58. Springer, Heidelberg, 2006.
- [3] G. ALLAIRE, E. BONNETIER, G. FRANCFORT, and F. JOUVE. Shape optimization by the homogenization method. Numer. Math., 76:2768, 1997.
- [4] G. ALLAIRE, F. JOUVE, and A.M. TOADER. Structural optimization using shape sensitivity analysis and a level-set method. Journal of Computational Physics, 194:363393, 2004.
- [5] M.P. BENDSØE. Methods for optimization of structural topology. In Shape and Material. Springer- Verlag, New York, 1995.
- [6] M.P. BENDSØE and N. KIKUCHI. Generating optimal topologies in structural design using a homogenization method. Computer Methods in Applied Mechanics and Engineering, 71:197224, 1988.
- [7] M.P. BENDSØE and O. SIGMUND. Topology Optimization, Theory, Methods and Applications. Springer Verlag, Berlin Heidelberg, 2nd edition, 2003.
- [8] M. BURGER. A framework for the construction of level-set methods for shape optimization and reconstruction. Interfaces and Free Boundaries, 5:301329, 2003.
- [9] J. CÉA Conception optimale ou identification de formes, calcul rapide de la dérivée directionnelle de la fonction coût Math. Model. Num., 3(20):371420, 1986.

- [10] C. DAPOGNY. Shape optimization, level set methods on unstructured meshes and mesh evolution. PhD thesis, Universite Pierre et Marie Curie, 2013.
- [11] C. DAPOGNY, P. FREY, F. OMNÈ and Y. PRIVAT. Geometrical shape optimization in fluid mechanics using freefem++. working paper or preprint, March 2017.
- [12] F. DE GOURNAY. Velocity extension for the level-set method and multiple eigenvalues in shape optimization. *SIAM J. on Control and Optim.*, 45(1):343367, 2006.
- [13] J. HADAMARD. Mémoire sur le problème d'analyse relatif à l'équilibre des plaque élastiques encastrées. Technical report, *Bull. Soc. Math. France*, 1907.
- [14] A. HENROT and M. PIERRE. *Variation et optimisation de formes, une analyse géométrique*. Springer, 2005.
- [15] C. KANE and M. SCHOENAUER. Topological optimum design using genetic algorithms. *Control and Cybernetics*, 25:10591088, 1996.
- [16] V.C. LE, H.T. PHAM, and T.T.M. Ta. Shape optimization for stokes flows using sensitivity analysis and finite element method. *Applied Numerical Mathematics*, 126:160 179, 2018.
- [17] F. MURAT and J. SIMON. *Sur le contrôle par un domaine géométrique Rr-76015*, INRIA Rocquencourt, 1976.
- [18] F. MURAT and S. SIMON. *Etudes de problèmes d'optimal design*, pages 5462. Springer Verlag, Berlin, 1976. *Lecture Notes in Computer Science* 41.
- [19] J. Simon. Differentiation with respect to the domain in boundary value problems. *Numer. Funct. Anal. Optim.*, 2:649687, 1980.
- [20] J. SOKOLOWSKI and J.-P. ZOLESIO. *Introduction to Shape Optimization; Shape Sensitivity Analysis*, volume 16 of *Series in Computational Mathematics*. Springer, Heidelberg, 1992.
- [21] T.T.M. TA. *Modélisation des problèmes bi-fluides par la méthode des lignes de niveaux et l'adaptation du maillage: Application à l'optimisation des formes*. PhD thesis, univ. Pierre et Marie Curie, 2015.
- [22] M.Y. WANG, X.M. WANG, and D.M. GUO. A level set method for structural topology optimization. *Computer Methods in Applied Mechanics and Engineering*, 192:227246, 2003.